Flavin Redox Chemistry Precedes Substrate Chlorination during the Reaction of the Flavin-Dependent Halogenase RebH†

Ellen Yeh,‡ Lindsay J. Cole,§ Eric W. Barr,|| J. Martin Bollinger, Jr.,|| David P. Ballou,§ and Christopher T. Walsh*,‡

Department of Biological Chemistry and Molecular Pharmacology, Harvard Medical School, Boston, Massachusetts 02115, Department of Biological Chemistry, University of Michigan, Ann Arbor, Michigan 48109, and Department of Biochemistry and Molecular Biology and Department of Chemistry, The Pennsylvania State University, University Park, Pennsylvania 16802

Received March 28, 2006; Revised Manuscript Received April 28, 2006

ABSTRACT: The flavin-dependent halogenase RebH catalyzes chlorination at the C7 position of tryptophan as the initial step in the biosynthesis of the chemotherapeutic agent rebeccamycin. The reaction requires reduced $FADH_2$ (provided by a partner flavin reductase), chloride ion, and oxygen as cosubstrates. Given the similarity of its sequence to those of flavoprotein monooxygenases and their common cosubstrate requirements, the reaction of $FADH_2$ and O_2 in the halogenase active site was presumed to form the typical FAD(C4a)−OOH intermediate observed in monooxygenase reactions. By using stopped-flow spectroscopy, formation of a FAD(C4a)−OOH intermediate was detected during the RebH reaction. This intermediate decayed to yield a FAD(C4a)−OH intermediate. The order of addition of $FADH_2$ and O_2 was critical for accumulation of the FAD(C4a)-OOH intermediate and for subsequent product formation, indicating that conformational dynamics may be important for protection of labile intermediates formed during the reaction. Formation of flavin intermediates did not require tryptophan, nor were their rates of formation affected by the presence of tryptophan, suggesting that tryptophan likely does not react directly with any flavin intermediates. Furthermore, although final oxidation to FAD occurred with a rate constant of 0.12 s^{-1}, quenched-flow kinetic data showed that the rate constant for 7-chlorotryptophan formation was 0.05 s^{-1} at 25 °C. The kinetic analysis establishes that substrate chlorination occurs after completion of flavin redox reactions. These findings are consistent with a mechanism whereby hypochlorite is generated in the RebH active site from the reaction of $FADH_2$, chloride ion, and O_2.

The enzyme RebH is a flavin-dependent halogenase that, along with its partner flavin reductase RebF, forms 7-chlorotryptophan as the first step in biosynthesis of the chemotherapeutic agent rebeccamycin, as shown in Scheme 1 (*1*, *2*). Members of this class of flavin-dependent halogenases are found in numerous gene clusters responsible for the biosynthesis of important natural products, such as the antibiotics chloramphenicol (*3*) and vancomycin (*4*) as well as the antifungal agent pyrrolnitrin (*5*, *6*). In many of these pathways, the halogenase likely acts as a tailoring enzyme on biosynthetic intermediates that are tethered on carrier protein domains of nonribosomal peptide synthetases and polyketide synthases (*7*, *8*).

In general, this class of flavin-dependent halogenases catalyzes the chlorination of electron-rich aromatic or heteroaromatic rings (*9*). The reaction carried out by the halogenase requires the reduced form of FAD,[1] chloride ion, and molecular oxygen as cosubstrates. $FADH_2$, generated by a separate flavin reductase, is bound by the halogenase and reacts with O_2, chloride ion, and substrate in the halogenase active site to form the chlorinated product (*6*). Several two-component flavin-dependent monooxygenases, which also use a separate reductase and oxygenase, have recently been described as well (*10*−*12*).

Given their sequence similarity and the common requirement for $FADH_2$ and O_2, the initial reaction of a flavin-dependent halogenase was thought to resemble that of a flavin monooxygenase. Flavin monooxygenases catalyze the reaction of $FADH_2$ and O_2 to form a FAD(C4a)−OOH intermediate (*13*). This versatile intermediate, which has been characterized in several systems by rapid-reaction spectroscopy, can be used for a diverse set of reactions. For example, in the prototypical flavin hydroxylase, *p*-hydroxybenzoate hydroxylase (PHBH), the FAD(C4a)−OOH intermediate provides a source of "OH^+" that is used to hydroxylate the aromatic substrate (*14*). By contrast, in the Baeyer−Villiger oxidation carried out by cyclohexanone monooxygenase, the FAD(C4a)−OO^- intermediate acts as a nucleophile to insert an O atom into the cyclohexanone ring (*15*, *16*). However, in the active site of the halogenase, the putative FAD(C4a)−OOH intermediate must be diverted to yield a chlorination outcome.

† This work was supported in part by NIH Grant GM 21643 (C.T.W.), NIH Grant GM 64711 (D.P.B.), and a NIH Medical Scientist Training Fellowship (E.Y.).

* To whom correspondence should be addressed: Harvard Medical School, 240 Longwood Ave., Boston, MA 02115. Telephone: (617) 432-1715. Fax: (617) 432-0438. E-mail: christopher_walsh@hms.harvard.edu.

‡ Harvard Medical School.

§ University of Michigan.

|| The Pennsylvania State University.

[1] Abbreviations: FAD, flavin adenine dinucleotide, oxidized form; $FADH_2$, flavin adenine dinucleotide, reduced form; NAD(P)H, β-nicotinamide adenine dinucleotide (phosphate), reduced form; PHBH, *p*-hydroxybenzoate hydroxylase; TLC, thin-layer chromatography; TCA, trichloroacetic acid.

10.1021/bi060607d CCC: $33.50
Published on Web 05/28/2006

Scheme 1: Formation of 7-Chlorotryptophan by RebH as the Initial Step of Rebeccamycin Biosynthesis[a]

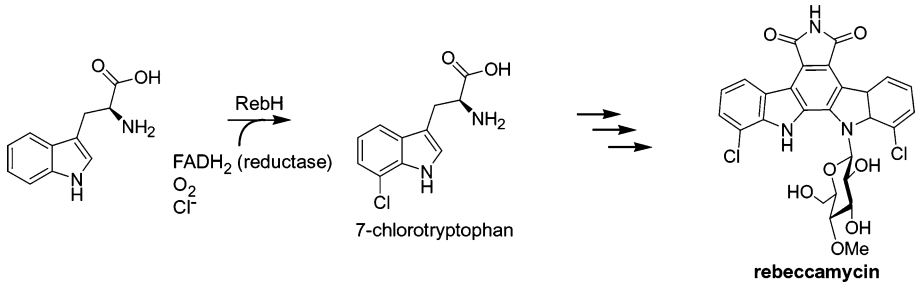

[a] RebH requires $FADH_2$ (provided by a flavin reductase), O_2, and Cl^- as cosubstrates.

Several mechanisms have been proposed for the C7 chlorination of tryptophan. One of these suggested the initial formation of an arene oxide form of tryptophan from its reaction with the FAD(C4a)−OOH intermediate (*6*). Chloride ion would then nucleophilically displace the O atom at C7 of the arene oxide intermediate to yield substrate chlorination. Two other mechanisms proposed the reaction of the FAD(C4a)−OOH intermediate with chloride ion to form an oxidized "Cl^+" equivalent, as either free HOCl or the FAD(C4a)−OCl intermediate (*2*, *17*). These chlorinating agents would then react via an electrophilic aromatic substitution of substrate tryptophan to yield the 7-chlorotryptophan product.

Recently, the crystal structure of PrnA, a tryptophan 7-halogenase from the pyrrolnitrin biosynthetic pathway with a sequence 53% identical and 67% similar to that of RebH, was determined (*17*). In the structure, the substrate tryptophan and bound FAD are 10 Å apart, precluding the direct reaction of tryptophan and any flavin intermediate, such as the FAD(C4a)−OOH intermediate or the proposed FAD(C4a)−OCl intermediate, during the reaction. Instead, the authors suggested that free hypochlorite, formed from the reaction of the FAD(C4a)−OOH intermediate with Cl^-, diffuses from its point of formation at the flavin to chlorinate bound tryptophan 10 Å away. From the structures that were obtained, there was no indication of any flavin movement that would be necessary to bring it into proximity with the tryptophan substrate to allow their direct reaction.

However, movement of the flavin cofactor and substrate is critical during the reaction of PHBH and phenol hydroxylase. The conformational dynamics of these enzymes have been extensively characterized (*18*−*27*). During the PHBH reaction, the flavin is shifted 7−8 Å from a solvent-protected *in* position (where oxygenation takes place) to an exposed *out* position (where NADPH can reduce the cofactor) (*20*, *21*). The FAD binding domain of PrnA is structurally quite similar to that of PHBH (*17*). Thus, a large conformational rearrangement of the halogenase during catalysis, although unlikely, cannot be ruled out. To gain insight into the chlorination reaction, we sought information about the kinetic behavior of the halogenase during catalysis to complement the evidence that is available from the structure.

In this study, we employed stopped-flow spectroscopy to characterize transient flavin intermediates in the RebH reaction and chemical quenched-flow methods to determine the kinetics of 7-chlorotryptophan formation. Our results demonstrate the formation of the proposed FAD(C4a)−OOH intermediate in the halogenase reaction and its decay to form a FAD(C4a)−OH intermediate. Addition of the substrate tryptophan had no effect on the spectral characteristics of these intermediates or on their rates of formation, indicating that tryptophan likely does not react directly with any flavin intermediates. However, formation of FAD(C4a) intermediates was dependent on the correct order of addition of $FADH_2$ and O_2 during the reaction, suggesting that significant protein dynamics occur during catalysis. These conformational changes are likely important for modulating the solvent accessibility of the active site and for protection of labile reaction intermediates. Finally, the formation of 7-chlorotryptophan was found to be rate-limiting in the overall reaction. The reaction kinetics demonstrate that substrate chlorination occurs after the redox reactions of the flavin are complete. This timing of flavin redox chemistry and substrate chlorination is consistent with a mechanism, recently suggested by the structure of the PrnA halogenase (*17*), in which hypochlorite is formed as a nascent product of flavin reactions in the halogenase active site.

MATERIALS AND METHODS

Preparation of the RebH Protein. Overexpression and purification of *N*-His_6-RebH was previously described (*2*). To reduce the amount of chloride ion introduced by buffer salts, the protein was purified by size-exclusion chromatography in 20 mM sodium phosphate buffer (pH 7.5). All reactions were carried out in this buffer. Care was taken to minimize introduction of chloride ion from glassware, the pH electrode, and other potential sources of contamination.

Stopped-Flow Analysis of Flavin Intermediates. Anaerobic solutions of FAD and/or enzyme containing 200 μM protocatechuate (3,4-dihydroxybenzoate) and 0.5 unit/mL protocatechuate 3,4-dioxygenase to remove trace amounts of O_2 were prepared in a glass tonometer and deoxygenated by repeated cycles of evacuation and purging with argon gas (*28*). Deoxygenated FAD was then reduced by titration with sodium dithionite. Solutions containing 121, 255, 607, and 1210 μM O_2 were prepared by being bubbled at 25 °C with 10, 21 (air), 50, and 100% O_2 gas, respectively. For the 1940 μM O_2 content, the solution was equilibrated at 4 °C with 100% O_2. All stopped-flow data were collected using a Hi-Tech Scientific model SF-61DX stopped-flow spectrophotometer in either absorbance or fluorescence mode. In single-mix mode, 50 μL of solution from each of two syringes were mixed in a reaction chamber for monitoring. In double-mix mode, 75 μL from each of the first two syringes were mixed and driven into an aging cylinder. In the second mix, this solution was mixed with an equal volume from a third syringe (90 μL each). Thus, in the observation chamber, each of the reactants from the first mix was diluted 4-fold, and

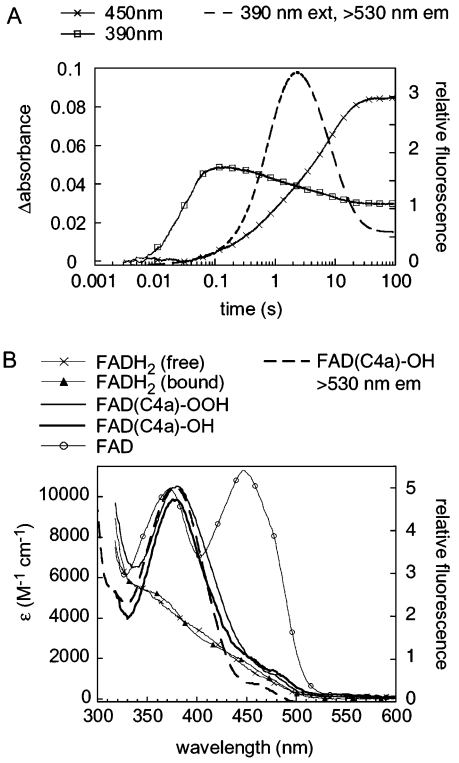

FIGURE 1: Formation of FAD(C4a)-oxygenated intermediates during the RebH reaction. (A) A solution containing 30 μM RebH, 121 μM O_2, and 10 mM NaCl was mixed with an equal volume of 15 μM $FADH_2$ at 25 °C. Reactions were monitored by absorbance at 390 (□) and 450 nm (×) and by fluorescence with excitation at 390 nm and detection at >530 nm (− − −). Fluorescence values are reported relative to that of FAD at 450 nm (its excitation maximum). (B) Spectra of species formed during the RebH reaction were derived from SVD analysis of the diode array data collected from 300 to 700 nm at 4 °C. Calculated absorbance spectra are shown for the bound complex of RebH·$FADH_2$ (▲), FAD(C4a)−OOH (gray line), and FAD(C4a)−OH (black line). Also shown is the fluorescence excitation spectrum of FAD(C4a)−OH (− − −), recorded approximately 15 s after mixing with detection at >530 nm emission. Free $FADH_2$ (×) and FAD (○) spectra are shown for comparison.

the reactant from the third syringe was diluted 2-fold. The final reaction from the second mix was monitored. Kinetic traces were analyzed and simulated with Kinetasyst 3 (Hi-Tech) and Program A (developed by R. Chang, C.-Y. Chiu, J. Dinverno, and D. Ballou, University of Michigan). Analysis is based upon the Marquardt algorithm for fitting data to sums of exponentials. All rate constants determined by this analysis had an error of no greater than ±10%. Spectra of intermediates were calculated by applying the rate constants determined from experiments with single-wavelength detection to singular-value decomposition (SVD) and multicomponent analysis of the diode array spectra using Specfit Global Analysis (Spectrum Software Associates). Modeling of the reaction kinetics for the formation of enzyme−flavin complexes was performed using Berkeley Madonna (developed by R. Macey and G. Oster, University of California, Berkeley, CA).

End-Point Assay for Single-Turnover Reactions. Formation of the 7-chlorotryptophan product was assessed under single-turnover conditions using different mixing procedures (analogous to reactions carried out in the stopped-flow instrument). The contents of syringe 1, as indicated in Figure 2B, were prepared in an MBraun Unilab glovebox kept at <2 ppm O_2. The protein sample was deoxygenated by size-exclusion chromatography on a Bio-Rad P-6DG column in O_2-free buffer [20 mM sodium phosphate (pH 7.5)]. All other chemicals were prepared from dry stock and dissolved in deoxygenated buffer. Sodium dithionite was used to reduce FAD. Anaerobic solutions were transferred from a sealed bottle using a gastight syringe and mixed with equal volumes of air-saturated solutions. Final reaction solutions (20 μL) contained 90 μM RebH, 20 μM $FADH_2$, 25 μM L-[^{14}C]Trp (53 Ci/mol), 5 mM NaCl, and 128 μM O_2 in 20 mM sodium phosphate buffer (pH 7.5). Reaction mixtures were incubated for 10 min at 25 °C and reactions quenched with TCA at a final concentration of 5%. Precipitated protein was removed by centrifugation. A 1.0 μL aliquot of each sample was spotted on a silica-C18 TLC plate (Sigma) and developed in 10% acetonitrile. Dried TLC plates were exposed for 12−16 h on BASIII imager plates (Fuji) and analyzed on a Typhoon 9200 phosphoimager (GE Healthcare). The ratio of L-Trp ($R_f = 0.59$) and 7-chlorotryptophan ($R_f = 0.2$) was calculated using ImageQuant version 5.2 to determine the fraction of substrate converted to product.

Kinetics of Product Formation by Rapid Chemical Quench. The kinetics of formation of 7-chlorotryptophan in single-turnover reactions were determined by chemical quench-flow techniques. As in end-point assays described above, anaerobic solutions were prepared in an MBraun Unilab glovebox and loaded into one syringe of an Update Instruments System 1000 chemical/freeze-quench apparatus. Air-saturated solutions were loaded in a second syringe of the instrument. During the experiment, actuation of the ram drive forced equal volumes from the two syringes to mix in a reaction hose. Final reaction concentrations were 40 μM RebH, 2.5 mM NaCl, 30 μM L-[^{14}C]Trp, 15 μM $FADH_2$, and 128 μM O_2. The reaction solution was passed through a reaction hose of a length appropriate to give the desired reaction time. The 50 μL reaction solution was mixed with 35 μL of 15% TCA in a reaction vial upon ejection. Product conversion was assessed by radio-TLC as described above for end-point assays. The rate constant for 7-chlorotryptophan formation was determined by plotting the fraction of product formed versus time and fitting the equation for single-exponential growth, $(A_f - A_0)(1 - e^{-kt}) + A_0$, where A_f is the final product yield and A_0 the background radioactivity, to the data.

RESULTS

Formation of FAD(C4a)-oxygenated Intermediates. Typically, the FAD(C4a)-oxygenated species, FAD(C4a)−OOH and FAD(C4a)−OH, detected in monooxygenase reactions have absorbance maxima between 370 and 400 nm (*13*). To test for the formation of such intermediates, RebH and NaCl in oxygenated solution were mixed with $FADH_2$ in a stopped-flow apparatus and monitored by either absorbance or fluorescence detection. Time courses of the reaction at 25 °C are shown in Figure 1A. Several phases were observed at 390 nm, suggesting formation of FAD(C4a)-oxygenated intermediates prior to formation of the final FAD form (observed at 450 nm). The large increase in the absorbance at 390 nm from ~10 to 100 ms is likely due to formation of FAD(C4a)−OOH from the reaction of $FADH_2$ and O_2. Conditions governing its formation and the oxygen depen-

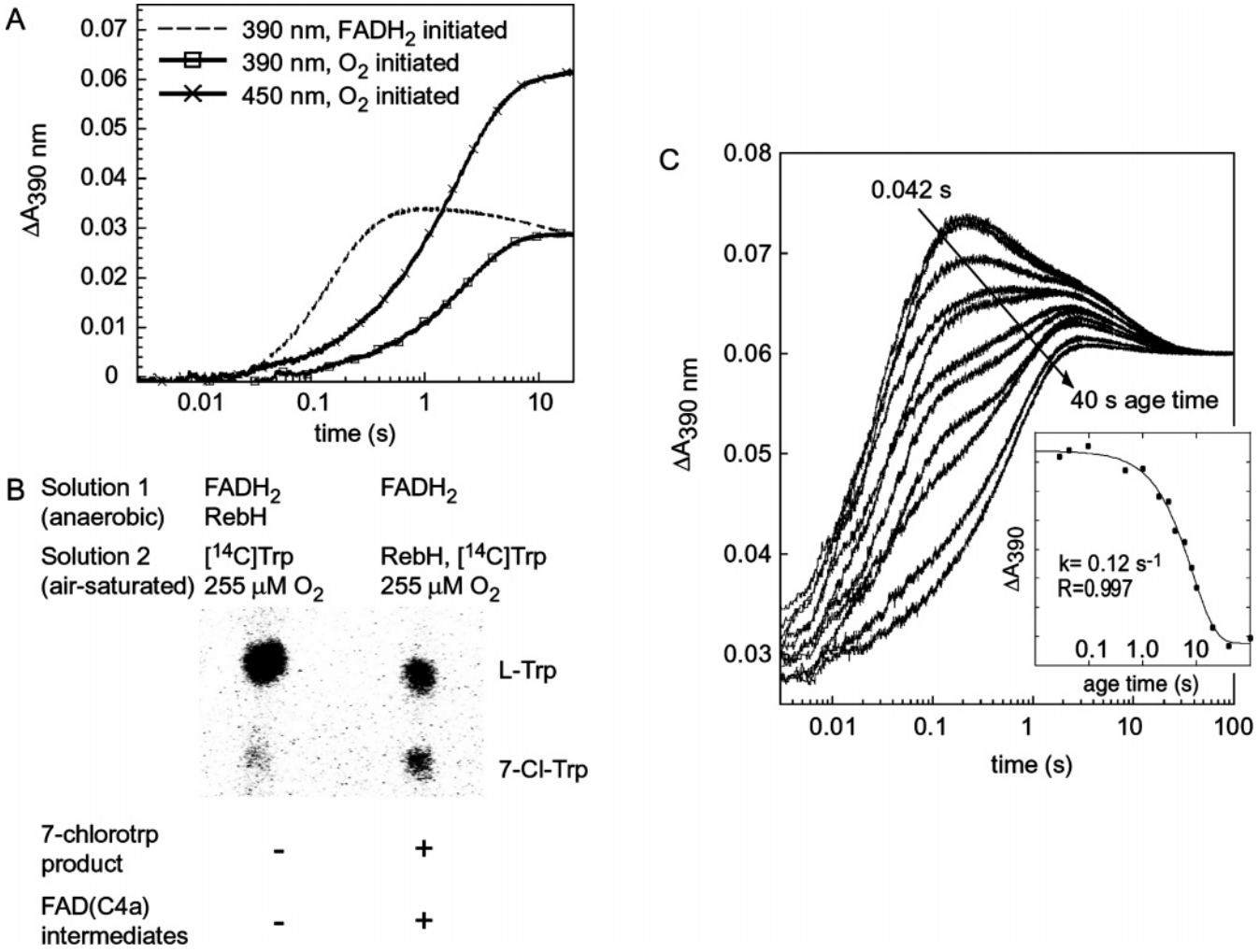

FIGURE 2: Order of addition of $FADH_2$ and O_2 determines formation of FAD(C4a) intermediates and 7-chlorotryptophan product. (A) Formation of FAD(C4a)-oxygenated intermediates using different mixing procedures was assessed. When 12 μM $FADH_2$ was mixed with a solution containing 30 μM RebH, 10 mM NaCl, and 255 μM O_2 at 4 °C, a rapid increase in absorbance at 390 nm (- - -) indicated formation of FAD(C4a) intermediates. However, when oxygenated buffer was added to an anaerobic solution of RebH and $FADH_2$, the absorbance at 390 nm (□) increased at the same rate as that at 450 nm (×), indicating formation of oxidized FAD with no observable accumulation of FAD(C4a) intermediates. (B) Formation of 7-chlorotryptophan from L-[^{14}C]Trp substrate was assessed for reactions initiated with O_2 (left) or $FADH_2$ (right). Anaerobic solution 1 was mixed with oxygenated solution 2 as indicated. Concentrations in the final reaction mix were 90 μM RebH, 18 μM $FADH_2$, 5 mM NaCl, 128 μM O_2, and 25 μM L-[^{14}C]Trp. Reactions were analyzed by separation on TLC followed by storage phosphor autoradiography. (C) Double-mix experiments were carried out to determine the kinetics of the conversion to the inactive complex following anaerobic incubation of RebH with $FADH_2$. First, equal volumes of 30 μM RebH and 20 μM $FADH_2$ were mixed at 25 °C under anaerobic conditions and allowed to incubate from 0.42 to 40 s. Following the aging period, O_2 was added to a final concentration of 60 μM, and the formation of FAD(C4a) intermediates was monitored at 390 nm absorbance. The inset shows the change in absorbance at 138 ms, the time when maximal FAD(C4a)−OOH is observed, plotted against the age time. A single-exponential decay was fitted to the data to obtain a rate of 0.12 s^{-1} for conversion to the inactive complex.

dence of its rate of formation will be elaborated in later sections. The species formed in the next phase (0.1−2.2 s) corresponds to a highly fluorescent intermediate detected using 390 nm excitation and emission at >530 nm. This intermediate precedes formation of the final oxidized FAD and is likely to be FAD(C4a)−OH, which can be distinguished from FAD(C4a)−OOH in several enzymatic systems by the high quantum yield of its fluorescence compared with the negligible fluorescence of FAD(C4a)−OOH (*29*−*31*). Both the change in fluorescence and the change in absorbance at 390 nm indicated formation of FAD(C4a)−OH with an observed rate constant of 1.2 s^{-1} at 25 °C (0.12 s^{-1} at 4 °C). Finally, an increase in the absorbance at 450 nm over the period from ~2 to 20 s, corresponding to a decrease in fluorescence intensity, indicated dehydration of FAD(C4a)−OH to form FAD with a rate constant of 0.12 s^{-1} at 25 °C (0.012 s^{-1} at 4 °C). Note all rate constants reported in this study have an uncertainty of less than ±10%.

Formation and decay of the FAD(C4a)−OOH intermediate and the fluorescent FAD(C4a)−OH species occurred with similar kinetics in the absence and presence of L-tryptophan up to 300 μM. This lack of an effect would suggest that tryptophan does not directly react with any of the flavin intermediates. As seen in Figure 1A, some FAD formed from ~0.1 to 2.2 s, concurrent with formation of FAD(C4a)−OH. The rate of FAD formation was independent of O_2 and, therefore, could not be due to oxidation of unbound $FADH_2$. Rather, FAD formation during this interval indicated uncoupling of the reaction in which FAD(C4a)−OOH breaks down to FAD and H_2O_2. Interestingly, the amount of uncoupling increased with an increase in the chloride concentration. The mechanism of this uncoupling is unclear.

The reactions were also followed at 4 °C using a diode array detector from 300 to 700 nm. The spectra of relevant reaction species, calculated by applying rates determined from experiments using single-wavelength detection to the diode array data, are shown in Figure 1B. The initial binding step caused a perturbation of the $FADH_2$ spectrum with absorbance changes at 370 and 400 nm resulting in a more resolved spectrum. Similar absorbance changes were observed upon binding of $FADH_2$ by the two-component *p*-hydroxyphenylacetate hydroxylase from *Acinetobacter baumanii* (J. Sucharitakul, personal communication). Both FAD(C4a)−OOH and FAD(C4a)−OH had absorbance maxima around 380 nm. FAD(C4a)−OOH was formed with a rate constant of 4.5 s^{-1} at an oxygen concentration of 128 μM; FAD(C4a)−OH was formed with a rate constant of 0.12 s^{-1}, and its dehydration to form oxidized FAD occurred with a rate constant of 0.012 s^{-1}. The excitation spectrum of FAD(C4a)−OH (>530 nm emission) at 15 s, when this species reaches its maximum concentration at 4 °C, is also shown. The FAD(C4a)−OH spectra were corrected for 25 and 50% oxidized FAD present in the absorption spectra and fluorescence specta, respectively, from the breakdown of FAD(C4a)−OOH.

Order of Addition of $FADH_2$ and O_2. Formation of FAD(C4a)-oxygenated species was observed in the stopped flow when reactions were initiated by mixing $FADH_2$ from one syringe with enzyme and O_2 from a second syringe. However, when oxygenated buffer was mixed with an anaerobic solution of RebH and $FADH_2$, only a slow direct oxidation of bound $FADH_2$ to FAD ($k = 1.5 \times 10^3$ M^{-1} s^{-1} at 4 °C) was observed without buildup of FAD(C4a) intermediates (Figure 2A). The failure of FAD(C4a)−OOH to accumulate under these conditions correlated with a decreased yield of 7-chlorotryptophan, as monitored by radio-TLC using L-[^{14}C]tryptophan (Figure 2B). The results suggest that, following initial binding, a conformational change of the RebH·$FADH_2$ complex under anaerobic conditions prevents both generation of the active site FAD(C4a)−OOH and formation of chlorinated product.

To determine the kinetics of the conversion to this inactive conformation, a double-mix experiment was carried out in which anaerobic solutions of $FADH_2$ and RebH were combined in a first mix, allowed to incubate for time periods between 0.042 and 40 s, and then reacted with an oxygenated solution in a second mix. Formation of FAD(C4a)−OOH was quantified by the rapid phase of increase in absorbance at 390 nm. As shown in Figure 2C, the formation of FAD(C4a)−OOH was maximal with short age times (<100 ms at 25 °C) and decreased with longer anaerobic incubation times of $FADH_2$ and RebH. By plotting the amount of FAD(C4a)−OOH formed versus the age time and fitting the equation for a single-exponential decay to the data, we determined the rate constant for conversion to this inactive RebH·$FADH_2$ complex to be 0.12 s^{-1} at 25 °C (Figure 2C, inset). At 4 °C, the conversion to the inactive complex was 0.02 s^{-1}.

Dependence of FAD(C4a)−OOH Formation on O_2 Concentration. The reaction of RebH−$FADH_2$ complex and O_2 to form FAD(C4a)−OOH should be governed by a second-order rate constant dependent on both $FADH_2$ and O_2. However, when solutions of RebH and NaCl in oxygenated buffer were mixed with anaerobic solutions of $FADH_2$, the first-order rate constant of FAD(C4a)−OOH formation was 5.5 s^{-1} at 4 °C (39 s^{-1} at 25 °C) and did not vary with the final O_2 concentration from 60 to 970 μM. The O_2 dependence of the reaction rate could be masked by a slow reaction (e.g., binding or a protein conformational change) that precedes a faster O_2-dependent chemical reaction leading to formation of FAD(C4a)−OOH.

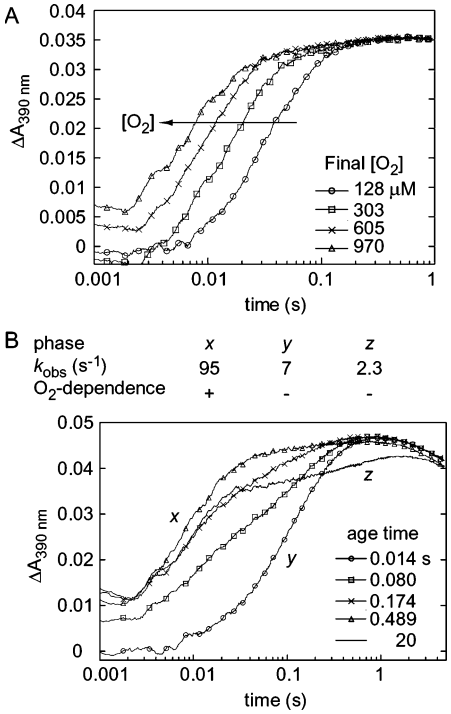

FIGURE 3: Dependence of FAD(C4a)−OOH formation on the O_2 concentration. (A) O_2-dependent rates of formation of FAD(C4a)−OOH were revealed using a double-mix procedure carried out at 4 °C. Solutions of 30 μM RebH and 20 μM $FADH_2$ were combined in a first mix and incubated for 0.5 s. Solutions containing 121−1940 μM O_2 were added in a second mix. Absorbance was monitored at 390 nm. (B) Additional O_2-independent phases were observed during the reaction forming FAD(C4a)−OOH when age times were varied from 0.014 to 20 s at 4 °C. Reactions were carried out as described for panel A with a 1940 μM O_2 solution added in the second mix. At the shortest age time of 0.014 s (○), a majority of FAD(C4a)−OOH formation occurred in phase *y*, which was attributed to slow binding of $FADH_2$ to RebH. As the age time was increased to 0.489 s (△), most of the FAD(C4a)−OOH intermediate was formed at a fast O_2-dependent rate designated phase *x*. When the age time was increased to 20 s (—), phase *z* appears. This additional O_2-independent rate indicated another step involving a conformational change of the enzyme bound to $FADH_2$.

Double-mix stopped-flow experiments were undertaken to parse the steps of the reaction leading to formation of FAD(C4a)−OOH. As before, anaerobic mixtures of RebH and $FADH_2$ were first incubated for short age times before introduction of O_2 in a second mix. Experiments carried out at 4 °C, which gave a better resolution for the fast O_2 reaction, are shown in Figure 3A. With a 500 ms age time [which gave the highest yield of the FAD(C4a) intermediate], the rate of formation of FAD(C4a)−OOH was dependent on the O_2 concentration with observed rates of 30.4 (128 μM), 65 (303 μM), 95 (605 μM), and 158 s^{-1} (970 μM) (final O_2 concentrations indicated). At 25 °C and an age time of 15 ms, rates of 45 (60 μM), 94 (128 μM), 207 (303 μM), and 388 s^{-1} (605 μM) were observed. Second-order rate

constants were calculated: 1.5×10^5 M^{-1} s^{-1} at 4 °C and 6.3×10^5 M^{-1} s^{-1} at 25 °C.

By varying the age time during which RebH and $FADH_2$ were incubated anaerobically, we could resolve additional phases en route to formation of FAD(C4a)−OOH. At delay times of <500 ms, a phase with an oxygen-independent rate constant of 7 s^{-1} at 4 °C was apparent (Figure 3B). The amplitude of this slow phase decreased as the age time was increased up to 500 ms when a majority of the increase at 390 nm could be attributed to the O_2-dependent phase. To test whether this phase could be due to slow binding of $FADH_2$, RebH and $FADH_2$ were mixed anaerobically at the same concentrations as in the experiments described above, and the reactions were monitored at 370 nm (the absorbance at this wavelength increases slightly upon binding of $FADH_2$ by RebH as seen in Figure 1B). The absorbance increased with a k of 5.8 s^{-1} at 4 °C. Thus, the binding rate obtained by this procedure was consistent with the slow 7 s^{-1} phase observed in double-mix experiments and the 5.5 s^{-1} rate observed in single-mix experiments. At 4 °C, it appears the binding of $FADH_2$ to form an oxygen-reactive complex is rate-limiting en route to FAD(C4a)−OOH but fast enough to prevent nonenzymatic oxidation of $FADH_2$ by oxygen in solution. At 25 °C, the binding rate was considerably faster with a k_{obs} of 100 s^{-1}. Therefore, the binding step could not be the slow 39 s^{-1} rate that limited the formation of FAD(C4a)−OOH at 25 °C in single-mix experiments.

At an age time of >500 ms but before conversion to the inactive RebH·$FADH_2$ complex, which occurred with a $t_{1/2}$ of 35 s at 4 °C, another slow O_2-independent phase with a rate constant of ~2.3 s^{-1} could be detected (Figure 3B). The appearance of this phase suggests yet another conformation of the RebH·$FADH_2$ complex, one that does not react readily with oxygen but could convert to the oxygen-reactive complex to yield FAD(C4a)−OOH with the observed O_2-independent rate. At 4 °C, this phase cannot be observed until an age time of more than 500 ms had passed. However, at 25 °C, almost one-third of the amplitude at 390 nm could be attributed to this phase (which had a rate of 35 s^{-1}), even at the shortest delay time of 20 ms. Once this oxygen-unreactive RebH·$FADH_2$ complex accumulates, its conversion to the oxygen-reactive form at 35 s^{-1} is rate-limiting in the formation of FAD(C4a)−OOH at 25 °C.

Rate of 7-Chlorotryptophan Formation. To determine the timing of product formation relative to the transitions between flavin species, chemical quenched-flow experiments were undertaken to measure the rate of product formation during a single turnover at both 4 and 25 °C. Reactions were initiated by mixing an air-saturated solution containing RebH, NaCl, and L-[^{14}C]Trp and an anaerobic solution of $FADH_2$. Reactions were quenched at 0.05−500 s and analyzed by TLC followed by storage phosphor autoradiography. The fraction of starting substrate converted to product was plotted versus time, and the equation for a single-exponential growth was fit to the data to give rate constants of 0.05 ± 0.007 s^{-1} at 25 °C (Figure 4) and 0.009 ± 0.002 s^{-1} at 4 °C. Controls using oxidized FAD or O_2 to initiate the reaction yielded negligible amounts of product. The yield of 7-chlorotryptophan was only 61% of the initial (limiting) $FADH_2$ concentration, indicating that a significant portion of $FADH_2$ was lost to nonproductive oxidation. The low ratio of product to $FADH_2$ consumption is at least partly due to the uncoupling observed in stopped-flow experiments, in which FAD(C4a)−OOH decomposed to FAD and H_2O_2.

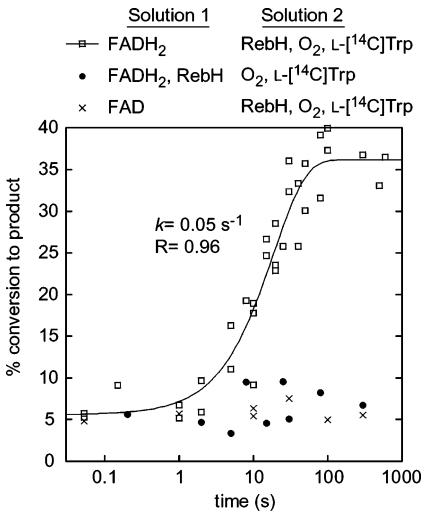

FIGURE 4: Rate of formation of 7-chlorotryptophan. Solutions were mixed using a quenched-flow apparatus at 25 °C as indicated. Final reaction mixtures contained 40 μM RebH, 2.5 mM NaCl, 30 μM L-[^{14}C]Trp, 15 μM $FADH_2$, and 128 μM O_2. Reactions were quenched at 0.05−500 s and analyzed by radio-TLC. Only $FADH_2$-initiated reactions gave significant yields of the 7-chlorotryptophan product (□). The fraction of starting substrate converted to product was plotted vs time, and the data were fitted to a single-exponential function to give a rate of 0.05 s^{-1}.

Scheme 2: Proposed RebH Reaction As Correlated with the Timing of Flavin Intermediates and Product Formation Observed at 25 °C

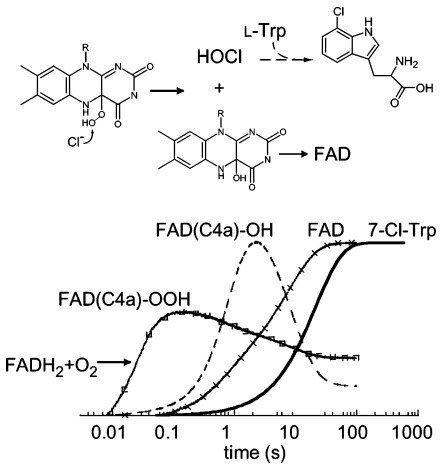

DISCUSSION

The observation that substrate chlorination occurs after the flavin reactions are complete rules out the direct chlorination of tryptophan by an oxidized flavin intermediate such as the

Scheme 3: Model of RebH and $FADH_2$ Binding and Complex Formation[a]

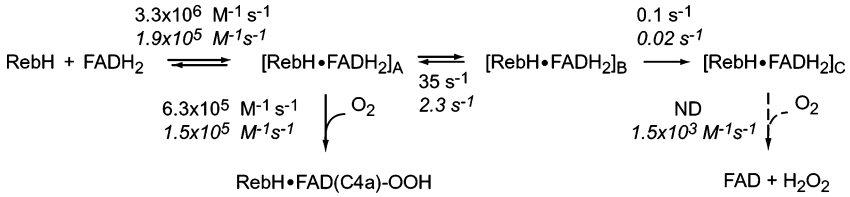

[a] Observed rates are indicated at both 25 and 4 °C.

proposed FAD(C4a)−OCl intermediate (*2*). Likewise, our study shows that tryptophan does not participate in reactions leading from $FADH_2$ to FAD(C4a)-oxygenated species to FAD, as the presence of tryptophan has no effect on the rates of formation or decay of FAD(C4a) intermediates. This evidence also excludes the proposed mechanism involving epoxidation of tryptophan by FAD(C4a)−OOH and subsequent reaction with Cl^- to form chlorinated product (*6*).

Instead, the mechanism of halogenation likely requires generation of an intermediary chlorinating agent, such as HOCl, produced from the flavin redox reactions. These kinetic results are in accordance with findings from a recently determined crystal structure of the related tryptophan 7-halogenase PrnA, which placed the flavin and substrate tryptophan 10 Å apart in the enzyme active site (*17*). A rather large conformational rearrangement would be required to bridge this distance and permit direct interaction of flavin and tryptophan during the enzyme reaction. In light of the results from kinetic analysis of RebH, this possibility appears even less likely.

The proposed reaction scheme for RebH, as it correlates with the spectroscopically observed species, is shown in Scheme 2. In this mechanism, the FAD(C4a)−OOH intermediate (observed as an increase in absorbance at 390 nm following mixing of RebH, $FADH_2$, and O_2) is captured by chloride ion on the distal oxygen such that an OH^+ equivalent is transferred to chloride ion to yield HOCl. With the transfer of the OH group, FAD(C4a)−OOH is thereby converted to FAD(C4a)−OH, observed as a second phase at 390 nm absorbance and, more clearly, as the appearance of a fluorescent species. Finally, dehydration of FAD(C4a)−OH yields fully oxidized FAD as observed by the increase in absorbance at 450 nm. Meanwhile, the actual chlorination of tryptophan occurs in a manner independent of the oxidative reactions of the flavin, and chlorinated product is not formed until after the flavin reactions are complete.

Neither the X-ray structure nor our kinetic analysis has been able to reveal the exact nature of the proximal chlorinating agent that reacts with tryptophan. The reactivity of HOCl is a major concern for generating such a species in the halogenase active site, as the enzyme must be able to control the substrate specificity and regiospecificity of chlorination. It was proposed from the PrnA structure that HOCl, once generated, enters a tunnel between the flavin cofactor and tryptophan (*17*). There, HOCl might hydrogen bond with the lysine 79 residue to position it for reaction at C7 of tryptophan. However, it is worth noting that amines are reactive with HOCl to form chloramines, and chloramines in turn are capable of directing a second chlorination (*32*, *33*). Thus, in principle, an enzyme chloramine intermediate formed on lysine 79 may be equally or perhaps better suited to serve as a regiospecific chlorinating agent.

The reaction kinetics for RebH also indicate that there are significant protein dynamics en route to formation of the FAD(C4a)−OOH intermediate. On the basis of our results, a model of the RebH−flavin interactions is proposed in Scheme 3. Three forms of the RebH·$FADH_2$ complex were detected with distinct oxygen reactivity and rates of interconversion. The initial binding of $FADH_2$ by RebH yields $(RebH{\cdot}FADH_2)_A$ which reacts readily with oxygen to form the FAD(C4a)−OOH intermediate. However, under anaerobic conditions, $(RebH{\cdot}FADH_2)_A$ converts reversibly to a second form, $(RebH{\cdot}FADH_2)_B$, and later to a third form, $(RebH{\cdot}FADH_2)_C$. Upon addition of O_2, the "B" form likely does not react readily with O_2 but primarily undergoes a moderately slow conversion back to "A" before reaction with O_2. By contrast, "C" is a dead-end complex, in that $FADH_2$ bound in this complex reacts with O_2 to form FAD and presumably H_2O_2 with no significant accumulation of FAD(C4a) intermediates or chlorinated product. The presence of $(RebH{\cdot}FADH_2)_B$ was suggested by the second, oxygen-independent phase observed in the double-mix experiments (Figure 3B). Evidence for the dead-end complex, $(RebH{\cdot}FADH_2)_C$, is clear from the dependence of the reaction on the order of addition of $FADH_2$ and O_2 (Figure 2).

Protein dynamics have been shown to be critical in catalysis by flavin monooxygenases (*25*). PHBH, which has a FAD binding domain that is structurally similar to that in the PrnA halogenase, adopts three conformations that have been detected by X-ray crystallography and kinetic analyses of wild-type and variant enzymes (*18*−*23*). An *out* conformation allows NADPH to access the exposed flavin and initiate the PHBH reaction by reducing the isoalloxazine ring. An *in* conformation shields the flavin from solvent, thus protecting the reactive FAD(C4a)−OOH intermediate formed when $FADH_2$ reacts with O_2. Finally, an *open* conformation permits trafficking of substrate and product in and out of the active site. These dynamic properties afford multiple sites for carrying out separate phases of catalysis, thereby optimizing each step in the reaction pathway. Although two-component monooxygenases separate the reduction of the flavin from the oxygenation reactions by using separate proteins, it nevertheless appears that protein dynamics are important in their catalysis. Recent characterization of the two-component *p*-hydroxyphenylacetate hydroxylase from *Acinetobacter baumannii* and *Pseudomonas aeruginosa* demonstrates long-lived FAD(C4a)−OOH intermediates ($t_{1/2}$ ∼ 80 s) that formed in the absence of substrate (*25*). In bacterial luciferase, the half-life of the FMN(C4a)−OOH intermediate was as long as 90 min at 0 °C (*34*). It is reasonable to assume that these enzymes also utilize shielded conformers to prevent access of the solvent to the reactive intermediate. Comparison of the substrate and product complex of the flavin halogenase PrnA, the sequence of

which is 53% identical and 67% similar to that of RebH, also points to the involvement of structural dynamics during substrate binding and reaction (*17*).

Analogous to the *in*, *out*, and *open* conformations of PHBH, the additional B and C conformations detected in the kinetic analysis of RebH might represent distinct protein−flavin complexes that are important for catalysis. Under aerobic conditions, binding of flavin is followed immediately by reaction with oxygen to form FAD(C4a)−OOH. Associated conformational changes may be involved in shielding oxygenated FAD(C4a) intermediates from solvent, thereby preventing their rapid breakdown and providing a site for generating the chlorinating agent. However, under anaerobic conditions, the formation of these highly shielded forms prevents subsequent reaction with O_2 to form oxygenated flavin intermediates. Hence, the availability of O_2 in the cell is critical during biosynthesis of the secondary metabolite. It is noted that the crystals of PrnA with bound FAD and Trp were obtained under aerobic conditions (*17*). If it adopts multiple conformations as observed in RebH, the solved PrnA structure may represent the "A" conformation at the start of the reaction or a product complex at the end of the reaction. It will be interesting to see how the conformations adopted during reaction differ from this structure. Investigation of these dynamics and their role in generating and controlling reactivity of the critical FAD(C4a)−OOH intermediate will require identification and study of variants that stabilize alternative conformations.

REFERENCES

1. Sanchez, C., Butovich, I. A., Brana, A. F., Rohr, J., Mendez, C., and Salas, J. A. (2002) The biosynthetic gene cluster for the antitumor rebeccamycin: Characterization and generation of indolocarbazole derivatives, *Chem. Biol. 9*, 519−531.
2. Yeh, E., Garneau, S., and Walsh, C. T. (2005) Robust in vitro activity of RebF and RebH, a two-component reductase/halogenase, generating 7-chlorotryptophan during rebeccamycin biosynthesis, *Proc. Natl. Acad. Sci. U.S.A. 102*, 3960−3965.
3. Piraee, M., White, R. L., and Vining, L. C. (2004) Biosynthesis of the dichloroacetyl component of chloramphenicol in *Streptomyces venezuelae* ISP5230: Genes required for halogenation, *Microbiology 150*, 85−94.
4. van Wageningen, A. M., Kirkpatrick, P. N., Williams, D. H., Harris, B. R., Kershaw, J. K., Lennard, N. J., Jones, M., Jones, S. J., and Solenberg, P. J. (1998) Sequencing and analysis of genes involved in the biosynthesis of a vancomycin group antibiotic, *Chem. Biol. 5*, 155−162.
5. Kirner, S., Hammer, P. E., Hill, D. S., Altmann, A., Fischer, I., Weislo, L. J., Lanahan, M., van Pee, K. H., and Ligon, J. M. (1998) Functions encoded by pyrrolnitrin biosynthetic genes from *Pseudomonas fluorescens*, *J. Bacteriol. 180*, 1939−1943.
6. Keller, S., Wage, T., Hohaus, K., Holzer, M., Eichhorn, E., and van Pee, K. H. (2000) Purification and partial characterization of tryptophan 7-halogenase (PrnA) from *Pseudomonas fluorescens*, *Angew. Chem., Int. Ed. 39*, 2300−2302.
7. Puk, O., Bischoff, D., Kittel, C., Pelzer, S., Weist, S., Stegmann, E., Sussmuth, R. D., and Wohlleben, W. (2004) Biosynthesis of chloro-*β*-hydroxytyrosine, a nonproteinogenic amino acid of the peptidic backbone of glycopeptide antibiotics, *J. Bacteriol. 186*, 6093−6100.
8. Dorrestein, P. C., Yeh, E., Garneau-Tsodikova, S., Kelleher, N. L., and Walsh, C. T. (2005) Dichlorination of a pyrrolyl-S-carrier protein by $FADH_2$-dependent halogenase PltA during pyoluteorin biosynthesis, *Proc. Natl. Acad. Sci. U.S.A. 102*, 13843−13848.
9. Vaillancourt, F. H., Yeh, E., Vosburg, D. A., Garneau-Tsodikova, S., and Walsh, C. T. (2006) Nature's inventory of halogenation catalysts, *Chem. Rev. 106*, in press.
10. Uetz, T., Schneider, R., Snozzi, M., and Egli, T. (1992) Purification and characterization of a two-component monooxygenase that hydroxylates nitrilotriacetate from "Chelatobacter" strain ATCC 29600, *J. Bacteriol. 174*, 1179−1188.
11. Prieto, M. A., and Garcia, J. L. (1994) Molecular characterization of 4-hydroxyphenylacetate 3-hydroxylase of *Escherichia coli*. A two-protein component enzyme, *J. Biol. Chem. 269*, 22823−22829.
12. Galan, B., Diaz, E., Prieto, M. A., and Garcia, J. L. (2000) Functional analysis of the small component of the 4-hydroxyphenylacetate 3-monooxygenase of *Escherichia coli* W: A prototype of a new Flavin:NAD(P)H reductase subfamily, *J. Bacteriol. 182*, 627−636.
13. Massey, V. (1994) Activation of molecular oxygen by flavins and flavoproteins, *J. Biol. Chem. 269*, 22459−22462.
14. Entsch, B., and van Berkel, W. J. (1995) Structure and mechanism of para-hydroxybenzoate hydroxylase, *FASEB J. 9*, 476−483.
15. Ryerson, C. C., Ballou, D. P., and Walsh, C. (1982) Mechanistic studies on cyclohexanone oxygenase, *Biochemistry 21*, 2644−2655.
16. Sheng, D., Ballou, D. P., and Massey, V. (2001) Mechanistic studies of cyclohexanone monooxygenase: Chemical properties of intermediates involved in catalysis, *Biochemistry 40*, 11156−11167.
17. Dong, C., Flecks, S., Unversucht, S., Haupt, C., van Pee, K. H., and Naismith, J. H. (2005) Tryptophan 7-halogenase (PrnA) structure suggests a mechanism for regioselective chlorination, *Science 309*, 2216−2219.
18. Palfey, B. A., Moran, G. R., Entsch, B., Ballou, D. P., and Massey, V. (1999) Substrate recognition by "password" in p-hydroxybenzoate hydroxylase, *Biochemistry 38*, 1153−1158.
19. Palfey, B. A., Ballou, D. P., and Massey, V. (1997) Flavin conformational changes in the catalytic cycle of p-hydroxybenzoate hydroxylase substituted with 6-azido- and 6-aminoflavin adenine dinucleotide, *Biochemistry 36*, 15713−15723.
20. Gatti, D. L., Palfey, B. A., Lah, M. S., Entsch, B., Massey, V., Ballou, D. P., and Ludwig, M. L. (1994) The mobile flavin of 4-OH benzoate hydroxylase, *Science 266*, 110−114.
21. Schreuder, H. A., Mattevi, A., Obmolova, G., Kalk, K. H., Hol, W. G., van der Bolt, F. J., and van Berkel, W. J. (1994) Crystal structures of wild-type p-hydroxybenzoate hydroxylase complexed with 4-aminobenzoate, 2,4-dihydroxybenzoate, and 2-hydroxy-4-aminobenzoate and of the Tyr222Ala mutant complexed with 2-hydroxy-4-aminobenzoate. Evidence for a proton channel and a new binding mode of the flavin ring, *Biochemistry 33*, 10161−10170.
22. Moran, G. R., Entsch, B., Palfey, B. A., and Ballou, D. P. (1996) Evidence for flavin movement in the function of p-hydroxybenzoate hydroxylase from studies of the mutant Arg220Lys, *Biochemistry 35*, 9278−9285.
23. Cole, L. J., Entsch, B., Ortiz-Maldonado, M., and Ballou, D. P. (2005) Properties of p-hydroxybenzoate hydroxylase when stabilized in its open conformation, *Biochemistry 44*, 14807−14817.
24. Brender, J. R., Dertouzos, J., Ballou, D. P., Massey, V., Palfey, B. A., Entsch, B., Steel, D. G., and Gafni, A. (2005) Conformational dynamics of the isoalloxazine in substrate-free p-hydroxybenzoate hydroxylase: Single-molecule studies, *J. Am. Chem. Soc. 127*, 18171−18178.
25. Ballou, D. P., Entsch, B., and Cole, L. J. (2005) Dynamics involved in catalysis by single-component and two-component flavin-dependent aromatic hydroxylases, *Biochem. Biophys. Res. Commun. 338*, 590−598.
26. Enroth, C., Neujahr, H., Schneider, G., and Lindqvist, Y. (1998) The crystal structure of phenol hydroxylase in complex with FAD and phenol provides evidence for a concerted conformational change in the enzyme and its cofactor during catalysis, *Structure 6*, 605−617.
27. Xu, D., Ballou, D. P., and Massey, V. (2001) Studies of the mechanism of phenol hydroxylase: Mutants Tyr289Phe, Asp54Asn, and Arg281Met, *Biochemistry 40*, 12369−12378.
28. Patil, P. V., and Ballou, D. P. (2000) The use of protocatechuate dioxygenase for maintaining anaerobic conditions in biochemical experiments, *Anal. Biochem. 286*, 187−192.
29. Moran, G. R., Entsch, B., Palfey, B. A., and Ballou, D. P. (1997) Electrostatic effects on substrate activation in para-hydroxyben-

zoate hydroxylase: Studies of the mutant lysine 297 methionine, *Biochemistry 36*, 7548−7556.
30. Ghisla, S., Entsch, B., Massey, V., and Husain, M. (1977) On the structure of flavin-oxygen intermediates involved in enzymatic reactions, *Eur. J. Biochem. 76*, 139−148.
31. Detmer, K., and Massey, V. (1984) Effect of monovalent anions on the mechanism of phenol hydroxylase, *J. Biol. Chem. 259*, 11265−11272.
32. Nightingale, Z. D., Lancha, A. H., Jr., Handelman, S. K., Dolnikowski, G. G., Busse, S. C., Dratz, E. A., Blumberg, J. B., and Handelman, G. J. (2000) Relative reactivity of lysine and other peptide-bound amino acids to oxidation by hypochlorite, *Free Radical Biol. Med. 29*, 425−433.
33. Bergt, C., Fu, X., Huq, N. P., Kao, J., and Heinecke, J. W. (2004) Lysine residues direct the chlorination of tyrosines in YXXK motifs of apolipoprotein A-I when hypochlorous acid oxidizes high-density lipoprotein, *J. Biol. Chem. 279*, 7856−7866.
34. Becvar, J. E., Tu, S. C., and Hastings, J. W. (1978) Activity and stability of the luciferase−flavin intermediate, *Biochemistry 17*, 1807−1812.

BI060607D